


Properties and synthesis of the superheavy nucleus $^{298}_{114}\text{Fl}$

Jia-Xing Li (李佳星),^{1,2} Wen-Xia Wang (王文霞),² and Hong-Fei Zhang (张鸿飞) ^{1,2,*}

¹*School of Physics, Xi'an Jiaotong University, 710049 Xi'an, People's Republic of China*

²*School of Nuclear Science and Technology, Lanzhou University, 730000 Lanzhou, People's Republic of China*



(Received 30 June 2022; accepted 19 August 2022; published 6 October 2022)

The one-nucleon separation energy S_n , two-nucleon separation energy S_{2n} , one-proton separation energy S_p , two-proton separation energy S_{2p} , α -decay energy Q_α , α -decay half-life and spontaneous fission half-life of $Z = 114$ isotopes and $N = 184$ isotones are calculated by the finite-range droplet model (FRDM2012). It is found that $N = 184$ is a neutron magic number, and $Z = 114$ is a proton magic number. The properties of $Z = 114$ isotopes and $N = 184$ isotones provide a vital signal that $^{298}_{114}\text{Fl}$ may be a spherical double-magic nucleus and also the center of the stability island of superheavy nuclei. Based on this, we began to investigate the optimal conditions for the synthesis of superheavy nucleus $^{298}_{114}\text{Fl}$ within the dinuclear system model. To produce such neutron-rich compound nucleus, we consider using the extremely neutron-rich radioactive beams to bombard actinide targets. The evaporation residue cross section of superheavy nuclei synthesized by radioactive beam is analyzed in detail. Finally, we suggest that for the synthesis of $^{298}_{114}\text{Fl}$, the radioactive beam-induced fusion reaction $^{64}\text{Ti} + ^{238}\text{U}$ in the $4n$ evaporation channel with an excitation energy of 43 MeV is optimal.

DOI: [10.1103/PhysRevC.106.044601](https://doi.org/10.1103/PhysRevC.106.044601)

I. INTRODUCTION

Since the theory predicted the existence of “island of stability” [1–3] in the 1960s, the properties and synthesis of superheavy nuclei (SHN) have always been a hot topic in the field of nuclear physics. With the progress of science and technology, great experimental success has been achieved during the past three decades. To date, SHN with $Z = 107–112$ have been synthesized by using cold fusion reactions at the GSI laboratory [4], while SHN with $Z = 113–118$ have been synthesized by using hot fusion reaction at Dubna and RIKEN [5,6]. The island of stability may be composed of hundreds of superheavy elements with relatively stable properties, and may be synthesized in the laboratory. However, the central position of the island of stability has not been observed in the laboratory. To accomplish this task, we must further understand the structural properties and synthesis mechanism of SHN. To precisely reproduce the experimental data, the reliability of basic nuclear data, such as the masses and deformations of colliding nuclei, are very important. In this work, we choose to use the FRDM2012 data [7], which are widely used. The data are composed of macroscopic droplet terms and a microscopic shell correction terms. The macroscopic term is calculated by using the finite-range droplet model (FRDM), while the shell term is calculated by using the folded-Yukawa single-particle potential. In general, the physical properties obtained by FRDM2012 provide a positive signal that $^{298}_{114}\text{Fl}$ [8,9] is the center of the stability island of SHN. Even if the stability cannot reach the level of ^{208}Pb , as long as its lifetime is not as fleeting as other similar elements,

we will certainly find the potential use of this superheavy element. It will no longer be a “mirage” that can only exist for a few milliseconds in the laboratory.

As we know, the ratio of neutron to proton of the heaviest known double magic nucleus ^{208}Pb is 1.54. The ratio of neutron to proton of the next double magic nucleus $^{298}_{114}\text{Fl}$ predicted by FRDM2012 is 1.61. Such a neutron-rich nuclide brings great difficulties for the laboratory to select the appropriate projectile-target combination to synthesize it. Currently, the vast majority of SHN synthesized in the laboratory are neutron deficient, and there is a gap in the SHN synthesized by cold fusion and those by hot fusion. Therefore, the research on synthesis of neutron-rich nuclei by radioactive beam is so meaningful that it can offer us some innovative ideas about the synthesis of $^{298}_{114}\text{Fl}$ and help us to find the center of the stability island of SHN. Nowadays, there are many modern radioactive-beam facilities [10–12], such as the Argonne Tandem Linac Accelerator System (ATLAS), the Facility for Rare Isotope Beams (FRIB), the Heavy Ion Research Facility in Lanzhou (HIRFL), and the Second Generation Production System of Online Accelerated Radioactive Ions (SPIRAL2) project of the French Large Heavy Ion Accelerator (GANIL). Although these modern radioactive-beam facilities can only produce weak-intensity beams, it is still necessary to systematically study the radioactive beam-induced fusion reaction, which will provide a lot of useful information for future experiments.

Our aim in this paper is to investigate the structural properties of $^{298}_{114}\text{Fl}$ and its synthesis mechanism. The paper is organized as follows: In Sec. II, the latest improved formula for calculating the α decay half-life proposed by Deng *et al.* is introduced. In addition, we also introduce an improved Swiatecki formula to calculate the spontaneous fission

* zhanghongfei@lzu.edu.cn

half-life of SHN. Finally, we describe the dinuclear system (DNS) model with sufficient ability to predict the evaporation residue cross section (ERCS) of fusion reactions. In Sec. III, we systematically calculate the one-nucleon separation energy S_n , two-nucleon separation energy S_{2n} , one-proton separation energy S_p , two-proton separation energy S_{2p} , α -decay energy Q_α , α -decay half-life, and spontaneous fission half-life of $Z = 114$ and $N = 184$ isotopes, which can be used as a powerful evidence to prove that the center of the stability island of SHN is ${}^{298}_{114}\text{Fl}$. The maximum ERCS of the optimal reaction for the synthesis of superheavy nucleus ${}^{298}_{114}\text{Fl}$ is discussed. The influence factors of ERCS of superheavy nuclei synthesized by radioactive beam are also analyzed. In Sec. IV, we summarize our work.

II. THEORETICAL FRAMEWORK

In experiment, α decay is the dominant decay mode of superheavy nuclei [13–19]. Therefore, detecting α -decay chains of synthesized superheavy nuclei is an important way to identify them [20,21]. In this paper, we use the improved Royer formula with only eight parameters, as proposed by Deng *et al.* [22]. This formula considers the contribution of centrifugal potential and the blocking effect of unpaired nucleons. It is more precise and simple than the original ones and its other improvements. The expression of the formula can be written as

$$\log_{10} T_{1/2} = a + bA^{1/6}\sqrt{Z} + c\frac{Z}{\sqrt{Q_\alpha}} + dl(l+1) + h, \quad (1)$$

where A , Z , and Q_α represent the mass number, proton number, and α -decay energy of parent nuclei. l is the angular momentum taken away by the α particle. The minimum angular momentum l_{\min} carried away by α particles can be obtained according to the conservation laws of angular momentum and parity. The values of the adjustable parameters are $a = -26.8125$, $b = -1.1255$, $c = 1.6057$, $d = 0.0513$. The values of h for different α -decay cases are expressed as

$$h = \begin{cases} 0 & \text{for even-even nuclei} \\ 0.3625 & \text{for even } Z, \text{ odd } N \text{ nuclei} \\ 0.2812 & \text{for odd } Z, \text{ even } N \text{ nuclei} \\ 0.7486 & \text{for doubly odd nuclei.} \end{cases} \quad (2)$$

The blocking effect h of the doubly odd nuclei is greater than that of the odd- A nuclei, because the doubly odd nuclei have two nucleons that are not paired and the odd- A nuclei have only one nucleon that is not paired.

Spontaneous fission is another common decay mode of SHN. It is a process in which a heavy nucleus spontaneously splits into two or more lighter nuclei, releasing several neutrons and generating huge energy when splitting. In the laboratory, spontaneous fission is one of the key factors affecting the lifetime of new superheavy elements and nuclides. Therefore, to better describe the structural properties of SHN, it is necessary to study its spontaneous fission. In this paper, we use an improved Swiatecki formula; the expression of the formula can be written as [23]

$$\log T_{1/2} = 1146.44 - 75.3153Z^2/A$$

$$\begin{aligned} & + 1.63792(Z^2/A)^2 - 0.0119827(Z^2/A)^3 \\ & + B_f(7.23613 - 0.0947022Z^2/A) \\ & + \begin{cases} 0, & Z \text{ and } N \text{ are even} \\ 1.53897, & A \text{ is odd} \\ 0.80822, & Z \text{ and } N \text{ are odd.} \end{cases} \quad (3) \end{aligned}$$

In this formula, Z is the proton number, N is the neutron number, and B_f is the theoretical shell correction value of the limited range droplet model FRDM2012.

Finally, we briefly introduce the DNS model [24–37]. The DNS model couples nucleon transfer with relative motion by solving a set of microscopically derived master equations (MEs) that distinguish protons and neutrons. Using this model, many teams have done a lot of work and verified its reliable prediction ability. In the DNS concept, the ERCS is expressed as [38]

$$\begin{aligned} \sigma_{ER}(E_{c.m.}) &= \frac{\pi \hbar^2}{2\mu E_{c.m.}} \sum_J (2J+1) T(E_{c.m.}, J) \\ &\quad \times P_{CN}(E_{c.m.}, J) W_{\text{sur}}(E_{c.m.}, J). \quad (4) \end{aligned}$$

In this formula, $E_{c.m.}$ is the center-of-mass incident energy, $T(E_{c.m.}, J)$ is the transmission probability of the system overcoming the Coulomb potential barrier to form a dinuclear system. $P_{CN}(E_{c.m.}, J)$ is the fusion probability. $W_{\text{sur}}(E_{c.m.}, J)$ is the survival probability of the formed compound nucleus, which can be estimated with a statistic model. The fusion dynamics are described as a diffusion process by numerically solving a set of two-variable MEs in the corresponding potential-energy surfaces. The time evolution of the distribution probability function, $P(Z_1, N_1, E_1, t)$, at time t to find Z_1 protons and N_1 neutrons in fragment 1 with excitation energy E_1 , it can be described by the following master equation:

$$\begin{aligned} & \frac{dP(Z_1, N_1, E_1, t)}{dt} \\ &= \sum_{Z'_1} W_{Z_1, N_1; Z'_1, N_1}(t) [d_{Z_1, N_1} P(Z'_1, N_1, E_1, t) \\ &\quad - d_{Z'_1, N_1} P(Z_1, N_1, E_1, t)] \\ &\quad + \sum_{N'_1} W_{Z_1, N_1; Z_1, N'_1}(t) [d_{Z_1, N_1} P(Z_1, N'_1, E_1, t) \\ &\quad - d_{Z_1, N'_1} P(Z_1, N_1, E_1, t)] \\ &\quad - \{\Lambda^{qf}[\Theta(t)] + \Lambda^{fs}[\Theta(t)]\} P(Z_1, N_1, E_1, t). \quad (5) \end{aligned}$$

Here $W_{Z_1, N_1; Z'_1, N_1}$ is the mean transition probability from the channel (Z_1, N_1) to (Z'_1, N_1) , while d_{N_1, Z_1} denotes the microscopic dimension corresponding to macroscopic state (Z_1, N_1) . All possible proton and neutron numbers of the fragment 1 is taken into the sum, but only one nucleon transfer is considered in the model ($N'_1 = N_1 \pm 1$, $Z'_1 = Z_1 \pm 1$). The evolution of the DNS along the distance between nuclei R leads to quasifission. The quasifission rate Λ^{qf} and fission rate Λ^{fs} are estimated with the one-dimensional Kramers formula. In Eq. (5), $W_{Z_1, N_1; Z'_1, N_1}$, d_{N_1, Z_1} , Λ^{qf} , and Λ^{fs} all depend on the local excitation energy of the DNS, which is defined as

$$e^* = E_x - U(N_1, Z_1, N_2, Z_2, R, \beta_1, \beta_2, J), \quad (6)$$

where the excitation energy E_x of the composite system is converted from the relative kinetic-energy loss, which is related to the Coulomb barrier and is determined for each initial relative angular momentum J by the parametrization method of the classical deflection function. $U(N_1, Z_1, N_2, Z_2, R, \beta_1, \beta_2, J)$ is the driving potential energy of the system for the nucleon transfer of the DNS, which is

$$\begin{aligned} U(N_1, Z_1, N_2, Z_2, R, \beta_1, \beta_2, J) &= B(N_1, Z_1, \beta_1) + B(N_2, Z_2, \beta_2) \\ &\quad - [B(N, Z, \beta) + V_{\text{rot}}^{\text{CN}}(J)] + U_C(Z_1, Z_2, \beta_1, \beta_2, R) \\ &\quad + U_N(N_1, Z_1, N_2, Z_2, R, \beta_1, \beta_2, J), \end{aligned} \quad (7)$$

where $N = N_1 + N_2$ and $Z = Z_1 + Z_2$. β_i ($i = 1, 2$) and β represent the quadrupole deformation of the two fragments and compound nucleus, respectively. R is the distance between nuclei at which the interaction potential between the two nuclei, $U_C + U_N$, has the minimum value. $B(N_1, Z_1, \beta_1)$, $B(N_2, Z_2, \beta_2)$, and $B(N, Z, \beta)$ are the binding energies of two deformed nuclei and compound nucleus, respectively. U_C , U_N , and $V_{\text{rot}}^{\text{CN}}$ are the nuclear, Coulomb interaction potential and the centrifugal energy, respectively.

III. RESULTS AND DISCUSSION

A. $Z = 114$ is the proton magic number

Through the separation energy, we can obtain information about the shell structure, especially the separation energy of two nucleons are useful for finding new magic numbers in superheavy nuclei. In addition, for superheavy nuclei, α decay is the main decay mode. α decay as an important probe for studying superheavy nuclei provides some important nuclear structure information. Therefore, it is also very important to determine the magic number by α -decay energy and α -decay half-life. Based on this, in Fig. 1, we systematically calculated the one-proton separation energy S_p , two-proton separation energy S_{2p} , α -decay energy Q_α and α -decay half-life of the $N = 184$ isotopic chain by the FRDM2012.

From Fig. 1(a), we notice that the values of S_p and S_{2p} show a decreasing trend with an increase in the proton number. In addition, S_p shows an obvious even-odd stagger effect. More importantly, it can be found that both have a larger downward slope between $Z = 114$ and $Z = 115$, implying that for the $N = 184$ isotopic chain, the $Z = 114$ nucleus is more stable. In Fig. 1(b), the calculated value of Q_α tend to increase with the increase of the proton number. It is worth noting that the value Q_α increases more dramatically as the proton number increases from 114 to 116. In Fig. 1(c), the calculated value of the α -decay half-life tends to decrease with the increase of the proton number. Its general trend is opposite to that of In Fig. 1(b), and the predicted α -decay half-life decreases sharply when the proton number Z is greater than 114. The strong shell effect once again verifies the conclusion that $Z = 114$ may be the proton magic number.

B. $N = 184$ is the nucleon magic number

In the above calculation, we get that $Z = 114$ may be a proton magic number. To find the center of the stability island

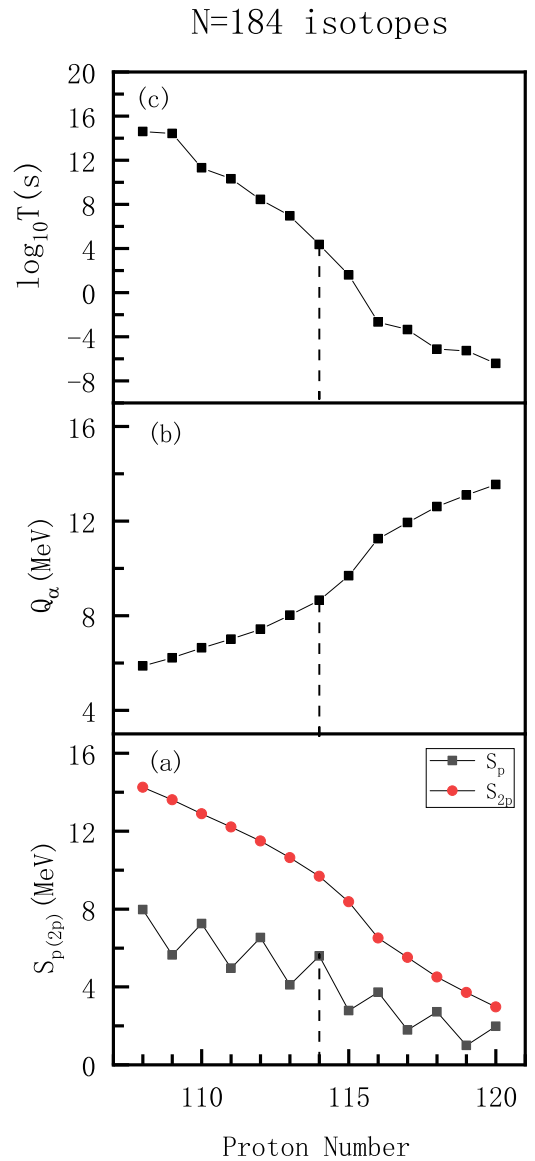


FIG. 1. (a) One and two proton separation energy, (b) α -decay energy Q_α , and (c) the α -decay half-life $\log_{10}T$ of the $N = 184$ isotopic chain.

of SHN accurately, we also calculated the one-neutron separation energy S_n , two-neutron separation energy S_{2n} , α -decay energy Q_α , and α -decay half-life of the $Z = 114$ isotopic chain in Fig. 2. The values of S_n and S_{2n} decrease with the increase of neutron number. S_n also shows an obvious even-odd stagger effect. In Fig. 2(a), it can be seen that both have a relatively large downward slope between $N = 184$ and $N = 185$, which means that, for the $Z = 114$ isotopic chain, the nucleus is more stable when the neutron number is 184. In Fig. 2(b), we find that, when $N = 184$, the slope of the α -decay energy curve begins to increase sharply. This change justifies that $N = 184$ may be the predicted neutron shell closure. In Fig. 2(c), when the neutron number N crosses $N = 184$, the predicted α decay half-life decrease sharply, and at $N = 186$, α decay half-life are reduced by more than three

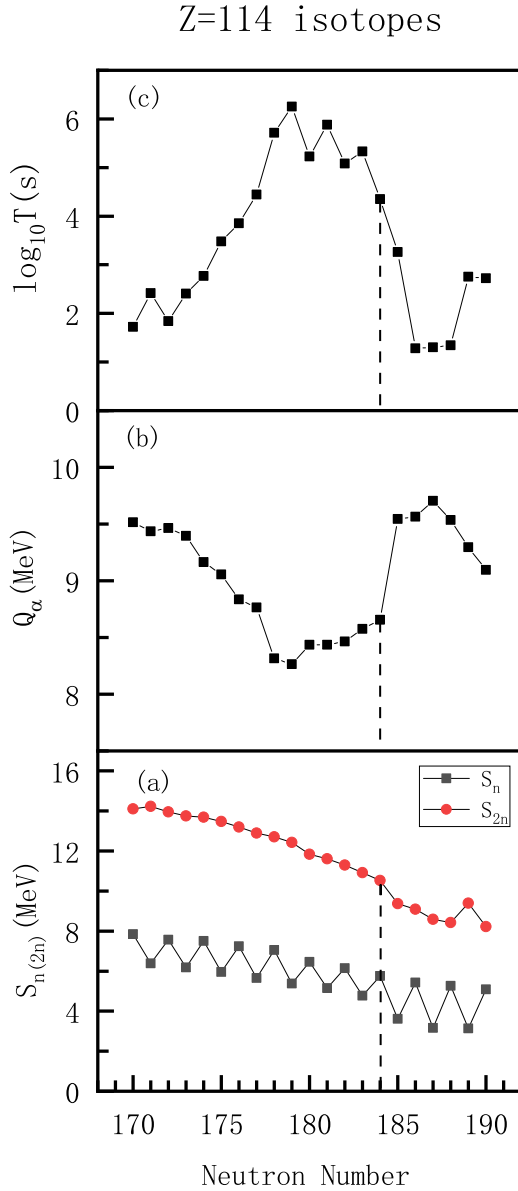


FIG. 2. (a) One and two nucleon separation energy, (b) α -decay energy Q_α , and (c) the α -decay half-life $\log_{10} T$ of the $Z = 114$ isotopic chain.

orders of magnitude. In short, there are signs that $N = 184$ may be the neutron magic number.

C. The center of the stability island of superheavy nuclei

Through the above analysis, we get that $Z = 114$ may be the proton magic number, and $N = 184$ is the neutron magic number. As we know, spontaneous fission half-life is one of the important indicators of the stability of SHN, which means whether the superheavy nuclei synthesized in the laboratory can survive stably. To verify that the center of the stability island of SHN is the double magic number nucleus $^{298}_{114}\text{Fl}$, we systematically calculated the spontaneous fission half-life of $N = 184$ isotopic chain and $Z = 114$ isotopic chain. In Fig. 3,

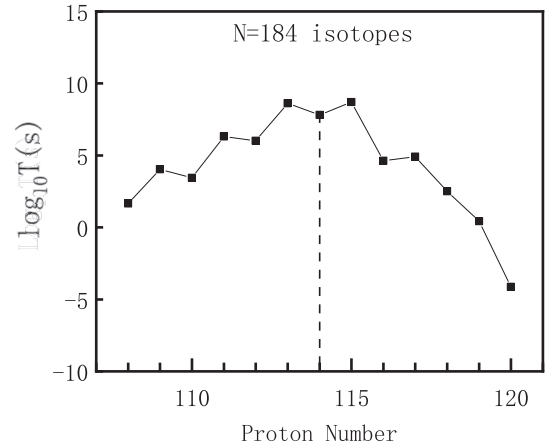


FIG. 3. Spontaneous fission half-life $\log_{10} T$ of $N = 184$ isotopic chain.

we can clearly see that for $N = 184$ isotopic chain, the spontaneous fission half-life first increases and then decreases with the increase of proton number Z , reaching the maximum near $Z = 114$. It is worth mentioning that the spontaneous fission half-life of odd A nuclei is greater than that of adjacent even-even nuclei, which is due to the odd nucleon effect. In Fig. 4, we can also observe that for $Z = 114$ isotopic chain, the spontaneous fission half-life is relatively long near $N = 184$. The calculation of spontaneous fission half-life once again shows that $^{298}_{114}\text{Fl}$ has more stable properties than other superheavy nuclei and is more likely to be the center of the stability island of SHN.

D. The evaporation residue cross section for synthesizing the double-magic nucleus $^{298}_{114}\text{Fl}$

In the study, we found that $^{298}_{114}\text{Fl}$ has a strong shell effect, which means that once the nuclide is synthesized in the laboratory, we will easily detect it. At present, some isotopes with $Z = 114$ have been synthesized in the laboratory by hot fusion

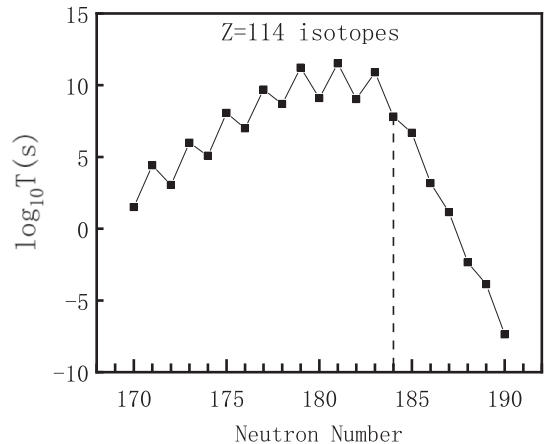


FIG. 4. Spontaneous fission half-life $\log_{10} T$ of $Z = 114$ isotopic chain.

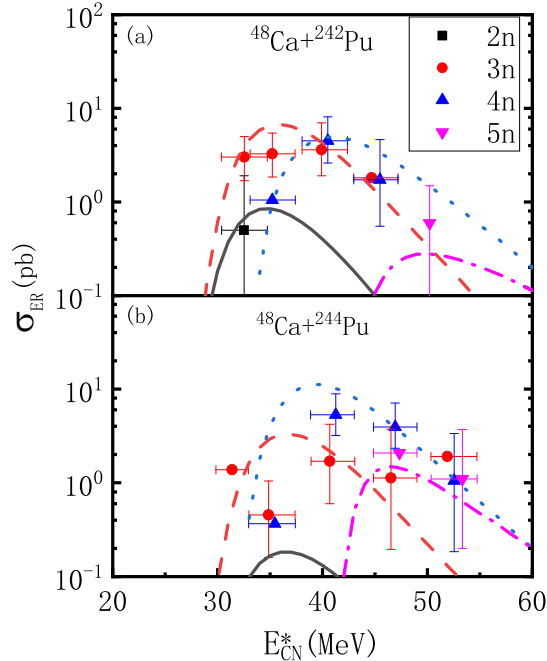


FIG. 5. Calculated ERCS compared with available experimental data [4,6]. Measured ERCS of the $2n$, $3n$, $4n$, and $5n$ channels are denoted by black square, red circle, blue normal triangle, and pink inverted triangle, respectively. Calculated results are denoted by black solid lines, red dashed lines, blue dotted lines, and pink dash-dotted lines, respectively.

reactions of ^{48}Ca with actinide targets. In Fig. 5, we calculated the ERCS for the $^{48}\text{Ca} + ^{242}\text{Pu} - ^{244}\text{Pu}$ reactions by the DNS model. The model, describing the dynamics of capture of the interacting nuclei, formation of an excited compound nucleus, and its final cooling down by the emission of neutrons reproduces reasonably accurately the measured ERCS in previous experiments. This directly shows the reliability of DNS model and provides a strong basis for us to study the synthesis conditions of ^{298}Fl .

For the synthesis of SHN $^{298}_{114}\text{Fl}$, the combination of stable nuclei cannot provide so many neutrons. Therefore, it is also necessary to study the synthesis mechanism of ^{298}Fl by radioactive beam induced hot fusion reaction. In some possible projectile-target combinations, we chose the reaction $^{64}\text{Ti} + ^{238}\text{U}$, because it has a relatively large ERCS. In Fig. 6, the calculated ERCS as a function of excitation energy is shown. We note that the maximal ERCS is 1.89 fb with an excitation energy of 43 MeV. Compared with the stable beam-induced fusion reactions, the radioactive beam-induced hot fusion reactions do not give much ERCS. More regrettably, the intensity of radioactive beam is lower than the intensity of the stable beam. However, it is undeniable that in order to synthesize neutron-rich superheavy nuclei, it is still a very promising way to use the radioactive-beam-induced hot fusion reactions.

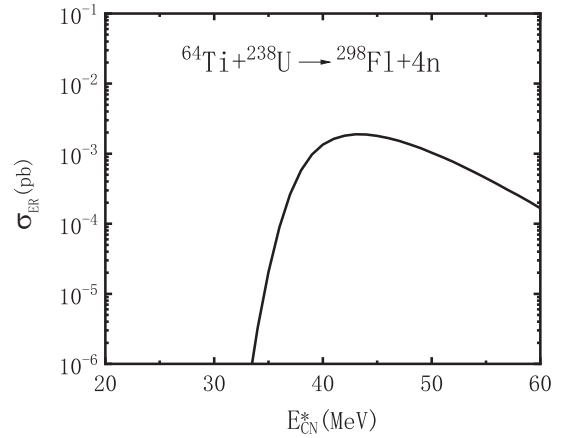


FIG. 6. The ERCS σ_{ER} as a function of excitation energy E_{CN}^* in the reaction $^{64}\text{Ti} + ^{238}\text{U}$.

E. Influencing factors of the evaporation residue cross section

As we know, the resulting ERCS depends on three processes: capture, fusion, and survival. Therefore, we show the capture cross section, fusion probability, survival probability as a function of excitation energy for the stable-beam-induced fusion reaction $^{48}\text{Ca} + ^{242}\text{Pu}$ and the radioactive-beam-induced reaction $^{64}\text{Ti} + ^{238}\text{U}$ in Fig. 7(a). In the lower excitation energy region, we notice that the capture cross section σ_{cap} increases with the increase of excitation energy. This is because the higher the excitation energy, the greater the possibility of overcoming the Coulomb barrier, and thus the capture cross section increases. In the higher excitation energy region, the capture cross section changes little with the excitation energy. In addition, the σ_{cap} for the reaction $^{48}\text{Ca} + ^{242}\text{Pu}$ is larger than $^{64}\text{Ti} + ^{238}\text{U}$, because of the relatively low Coulomb barrier of the former reaction. When the excitation energy $E_{CN}^* \geq 40$ MeV, the difference between them becomes smaller. In Fig. 7(b), we can see that the fusion probability P_{CN} increases with the increase of excitation energy. This is because, in the binuclear system, high excitation energy will lead to a large amount of energy dissipation, which will overcome the inner fusion barrier B_{fus} . In addition, we found that the fusion probability of reaction $^{48}\text{Ca} + ^{242}\text{Pu}$ is three orders of magnitude greater than that of reaction $^{64}\text{Ti} + ^{238}\text{U}$. To understand the reason, we calculated the driving potentials of the two reaction systems in Fig. 8. In the DNS model, fusion probability depends on the details of the driving potential, which is decided by the properties of the nuclei in each dinuclear system and their interactions. The hindrance in the diffusion process by nucleon transfer to form the compound nucleus is the inner fusion barrier B_{fus} , which is defined as the difference of the driving potential at the highest barrier called Businaro-Gallone (B.G.) point and at the entrance position. In other words, in order to occur a fusion reaction, the dinuclear system must overcome this potential barrier. The smaller the internal fusion barrier, the more conducive to the formation of compound nuclei. From Fig. 8, we can clearly see that the inner fusion barrier B_{fus} of reaction $^{48}\text{Ca} + ^{242}\text{Pu}$ is 8.78 MeV and that of reaction $^{64}\text{Ti} + ^{238}\text{U}$ is 13.4 MeV. Therefore, the reaction $^{48}\text{Ca} + ^{242}\text{Pu}$

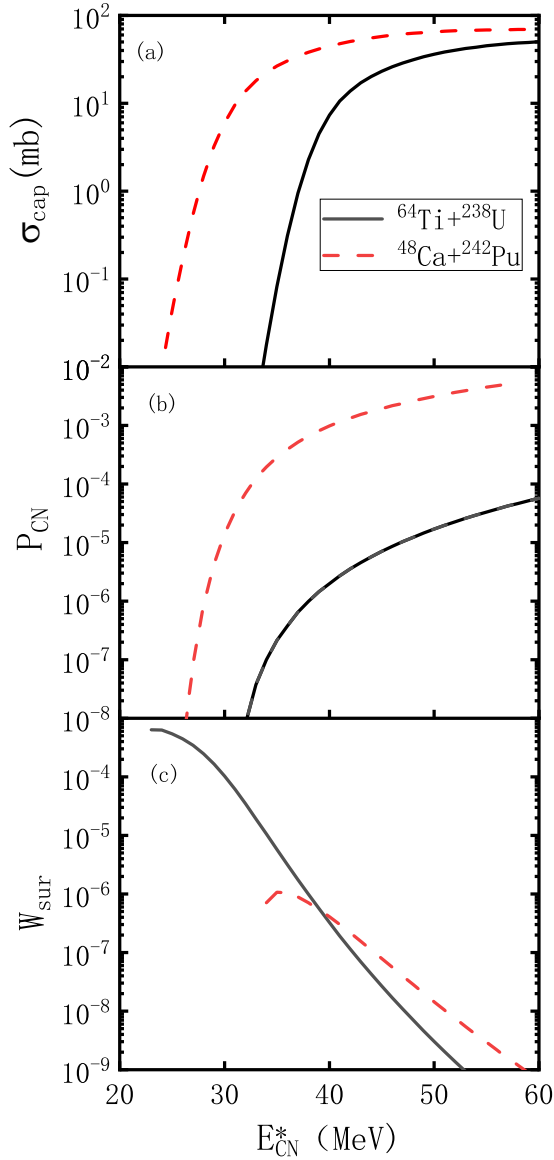


FIG. 7. (a) Capture cross sections are functions of excitation energy of compound nucleus. (b) Fusion probabilities are functions of excitation energy of compound nucleus. (c) Survival probabilities in the $4n$ channels are functions of excitation energy of compound nucleus.

is easier for the reaction $^{64}\text{Ti} + ^{238}\text{U}$ to overcome the internal fusion barrier B_{fus} and form a compound nucleus, and the fusion probability is greater.

Figure 7(c) shows the survival probability W_{sur} in the $4n$ channels as a function of the excitation energy of the compound nucleus. With the increase of excitation energy, the survival probability decreases, because high excitation energy will destroy the stability of compound nucleus, so that the survival probability becomes lower. In addition, survival probability is determined mainly by the difference between the fission-barrier height and neutron binding energy of the nuclei for each step of sequential neutron emission.

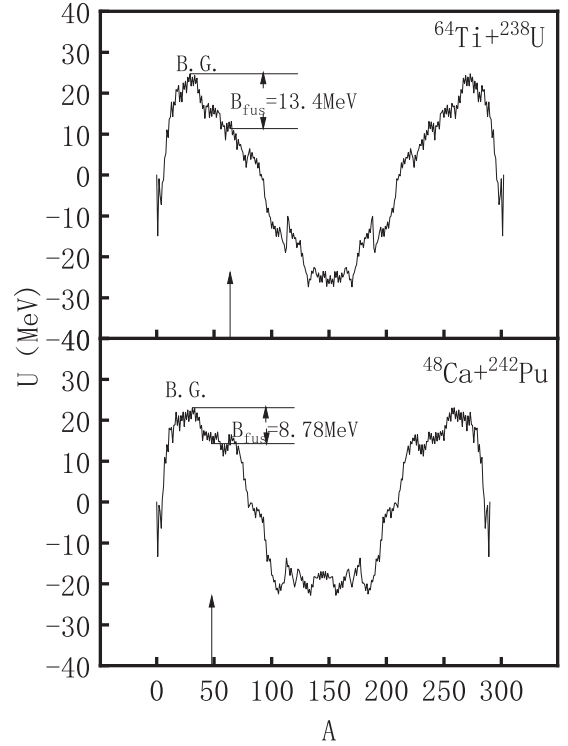


FIG. 8. The PES for the reaction $^{48}\text{Ca} + ^{242}\text{Pu}$ and $^{64}\text{Ti} + ^{238}\text{U}$ as functions of mass number A .

IV. SUMMARY

To find the next spherical double-magic nucleus, which is also the center of the stability island of SHN, we systematically calculated the structural properties of nuclides in $Z = 114$ isotopes and $N = 184$ isotones. Various signs show that $^{298}_{114}\text{Fl}$ is a spherical-double magic nucleus and the center of the stability island of SHN. For such a neutron rich nuclide as $^{298}_{114}\text{Fl}$, there is no stable projectile-target combination to synthesize it at present. Therefore, we propose to use the radioactive beam-induced hot fusion reaction $^{64}\text{Ti} + ^{238}\text{U}$ to complete the synthesis process. We obtain that the maximum ERCS is 1.89 fb, which appears when the excitation energy is 43 MeV in $4n$ evaporation channels. It is apparent that the ERCS of ^{64}Ti projectile is significantly reduced compared with ^{48}Ca -induced reactions. This is because, for the stable beam-induced fusion reaction $^{48}\text{Ca} + ^{242}\text{Pu}$, the fusion probability of the radioactive beam-induced reaction $^{64}\text{Ti} + ^{238}\text{U}$ is small, which is mainly due to its small mass asymmetry and large internal fusion barrier. Nevertheless, the use of radioactive beams to synthesize neutron-rich $^{298}_{114}\text{Fl}$ is still a very promising way. It is also hoped that some of the results and discussions in this paper can provide some help on the experimental synthesis of this new nuclide.

ACKNOWLEDGMENTS

This work is supported by National Natural Science Foundation of China (Grants No. 12175170 and No. 11675066.)

- [1] S. Hofmann and G. Münzenberg, *Rev. Mod. Phys.* **72**, 733 (2000).
- [2] S. Hofmann, *Prog. Part. Nucl. Phys.* **62**, 337 (2009).
- [3] Y. Z. Wang, S. J. Wang, Z. Y. Hou, and J. Z. Gu, *Phys. Rev. C* **92**, 064301 (2015).
- [4] Y. T. Oganessian, V. K. Utyonkov, Y. V. Lobanov, F. S. Abdullin, A. N. Polyakov, I. V. Shirokovsky, Y. S. Tsyganov, G. G. Gulbekian, S. L. Bogomolov, B. N. Gikal, A. N. Mezentsev, S. Iliev, V. G. Subbotin, A. M. Sukhov, A. A. Voinov, G. V. Buklanov, K. Subotic, V. I. Zagrebaev, M. G. Itkis, J. B. Patin *et al.*, *Phys. Rev. C* **69**, 054607 (2004).
- [5] Y. T. Oganessian, V. K. Utyonkov, Y. V. Lobanov, F. S. Abdullin, A. N. Polyakov, R. N. Sagaidak, I. V. Shirokovsky, Y. S. Tsyganov, A. A. Voinov, G. G. Gulbekian, S. L. Bogomolov, B. N. Gikal, A. N. Mezentsev, S. Iliev, V. G. Subbotin, A. M. Sukhov, K. Subotic, V. I. Zagrebaev, G. K. Vostokin, M. G. Itkis *et al.*, *Phys. Rev. C* **74**, 044602 (2006).
- [6] Y. T. Oganessian, V. K. Utyonkov, Y. V. Lobanov, F. S. Abdullin, A. N. Polyakov, I. V. Shirokovsky, Y. S. Tsyganov, G. G. Gulbekian, S. L. Bogomolov, B. N. Gikal, A. N. Mezentsev, S. Iliev, V. G. Subbotin, A. M. Sukhov, A. A. Voinov, G. V. Buklanov, K. Subotic, V. I. Zagrebaev, M. G. Itkis, J. B. Patin *et al.*, *Phys. Rev. C* **70**, 064609 (2004).
- [7] P. Miller, A. Sierk, T. Ichikawa, and H. Sagawa, *At. Data Nucl. Data Tables* **109-110**, 1 (2016).
- [8] P. A. Ellison, K. E. Gregorich, J. S. Berryman, D. L. Bleuel, R. M. Clark, I. Dragojević, J. Dvorak, P. Fallon, C. Fineman-Sotomayor, J. M. Gates, O. R. Gothe, I. Y. Lee, W. D. Loveland, J. P. McLaughlin, S. Paschalis, M. Petri, J. Qian, L. Stavsetra, M. Wiedeking, and H. Nitsche, *Phys. Rev. Lett.* **105**, 182701 (2010).
- [9] A. Sobczewski, F. Gareev, and B. Kalinkin, *Phys. Lett.* **22**, 500 (1966).
- [10] G. Savard, S. Baker, C. Davids, A. Levand, E. Moore, R. Pardo, R. Vondrasek, B. Zabransky, and G. Zinkann, *Nucl. Instrum. Methods Phys. Res., Sect. B* **266**, 4086 (2008).
- [11] W. Zhan, H. Xu, G. Xiao, J. Xia, H. Zhao, and Y. Yuan, *Nucl. Phys. A* **834**, 694c (2010).
- [12] S. Gales, *Prog. Part. Nucl. Phys.* **59**, 22 (2007).
- [13] W. M. Seif, *Phys. Rev. C* **74**, 034302 (2006).
- [14] J. Khuyagbaatar, A. Yakushev, C. E. Düllmann, D. Ackermann, L.-L. Andersson, M. Asai, M. Block, R. A. Boll, H. Brand, D. M. Cox, M. Dasgupta, X. Derks, A. Di Nitto, K. Eberhardt, J. Even, M. Evers, C. Fahlander, U. Forsberg, J. M. Gates, N. Gharibyan *et al.*, *Phys. Rev. Lett.* **112**, 172501 (2014).
- [15] R. J. Carroll, R. D. Page, D. T. Joss, J. Uusitalo, I. G. Darby, K. Andgren, B. Cederwall, S. Eeckhaudt, T. Grahn, C. Gray-Jones, P. T. Greenlees, B. Hadinia, P. M. Jones, R. Julin, S. Juutinen, M. Leino, A.-P. Leppänen, M. Nyman, D. O'Donnell, J. Pakarinen *et al.*, *Phys. Rev. Lett.* **112**, 092501 (2014).
- [16] W. M. Seif, M. Shalaby, and M. F. Alrakshy, *Phys. Rev. C* **84**, 064608 (2011).
- [17] Y. Ren and Z. Ren, *Phys. Rev. C* **85**, 044608 (2012).
- [18] Y. Qian, Z. Ren, and D. Ni, *Phys. Rev. C* **89**, 024318 (2014).
- [19] Z. Ren, *Phys. Rev. C* **65**, 051304(R) (2002).
- [20] Y. T. Oganessian, V. K. Utyonkov, Y. V. Lobanov, F. S. Abdullin, A. N. Polyakov, R. N. Sagaidak, I. V. Shirokovsky, Y. S. Tsyganov, A. A. Voinov, G. G. Gulbekian, S. L. Bogomolov, B. N. Gikal, A. N. Mezentsev, V. G. Subbotin, A. M. Sukhov, K. Subotic, V. I. Zagrebaev, G. K. Vostokin, M. G. Itkis, R. A. Henderson *et al.*, *Phys. Rev. C* **76**, 011601(R) (2007).
- [21] Y. T. Oganessian, *Radiochim. Acta* **99**, 429 (2011).
- [22] J.-G. Deng, H.-F. Zhang, and G. Royer, *Phys. Rev. C* **101**, 034307 (2020).
- [23] W. J. Swiatecki, *Phys. Rev.* **100**, 937 (1955).
- [24] G. G. Adamian, N. V. Antonenko, and W. Scheid, *Phys. Rev. C* **69**, 044601 (2004).
- [25] Z.-Q. Feng, G.-M. Jin, J.-Q. Li, and W. Scheid, *Phys. Rev. C* **76**, 044606 (2007).
- [26] N. Wang, J.-q. Li, and E.-g. Zhao, *Phys. Rev. C* **78**, 054607 (2008).
- [27] Z.-Q. Feng, G.-M. Jin, and J.-Q. Li, *Phys. Rev. C* **80**, 057601 (2009).
- [28] Z.-Q. Feng, G.-M. Jin, and J.-Q. Li, *Phys. Rev. C* **80**, 067601 (2009).
- [29] M. Huang, Z. Gan, X. Zhou, J. Li, and W. Scheid, *Phys. Rev. C* **82**, 044614 (2010).
- [30] M. Huang, Z. Zhang, Z. Gan, X. Zhou, J. Li, and W. Scheid, *Phys. Rev. C* **84**, 064619 (2011).
- [31] N. Wang, E.-G. Zhao, W. Scheid, and S.-G. Zhou, *Phys. Rev. C* **85**, 041601(R) (2012).
- [32] W. Nan, D. Liang, Z. En-Guang, and W. Scheid, *Chin. Phys. Lett.* **27**, 062502 (2010).
- [33] H. Ming-Hui, G. Zai-Guo, F. Zhao-Qing, Z. Xiao-Hong, and L. Jun-Qing, *Chin. Phys. Lett.* **25**, 1243 (2008).
- [34] G. Adamian, N. Antonenko, W. Scheid, and V. Volkov, *Nucl. Phys. A* **627**, 361 (1997).
- [35] G. Adamian, N. Antonenko, W. Scheid, and V. Volkov, *Nucl. Phys. A* **633**, 409 (1998).
- [36] J. Hong, G. Adamian, and N. Antonenko, *Phys. Lett. B* **764**, 42 (2017).
- [37] J.-X. Li and H.-F. Zhang, *Phys. Rev. C* **105**, 054606 (2022).
- [38] G. Adamian, N. Antonenko, and W. Scheid, *Nucl. Phys. A* **678**, 24 (2000).